HYDROELASTIC BEHAVIOR OF FLEXIBLE COMPOSITE PROPELLERS IN WAKE INFLOW

Yin L. Young
Department of Civil and Environmental Engineering, Princeton University

Keywords: *composite propeller, fluid-structure interaction, hydroelastic tailoring*

Abstract

In this work, a coupled boundary element method (BEM) – finite element method (FEM) is presented for the numerical analysis of flexible composite propellers in uniform flow and in wake inflow. An overview of the formulation for both the fluid and solid solvers, and the fluid-structure interaction algorithms are presented. The numerical predictions are compared with experimental measurements for a rigid and flexible composite propeller pair tested at the Naval Surface Warfare Center, Carderock Division. Both experimental and numerical studies showed that the load-dependent bending-twisting coupling behavior of anisotropic composites can be exploited to improve propeller efficiency via passively hydroelastic tailoring.

1 Introduction

Recently, there is an increased interest to use composites as alternative materials for marine propellers. Composite propellers can significantly reduce the weight to increase payload, and has the potential to eliminate the galvanic cell set up to dramatically lower corrosion of steel ships and life time costs [1]. In addition, another important feature of composite marine propellers is the possibility for passive hydroelastic tailoring by exploiting the bending-twisting coupling effects of anisotropic composite laminates. The load-dependent blade deformations of a flexible composite propeller can be tailored to reduce load variations, delay cavitation inception, and improve propeller efficiency by automatically adjusting the blade shape in wake inflow or in off-design conditions.

Although performance tests of composite propellers have been conducted on a range of naval vessels since the 1980s, much of the scientific information is not available in open literature [2]. According to studies shown in [3-7], the hydrodynamic performance of composite propellers is approximately the same as their metallic counterparts, but they offer the added benefits of weight reduction, lowered production cost, smoother take-up of power, reduced noise, reduced blade vibration, and better fatigue performance. However, except for a few cases, most of these composite propellers were designed to be the same as their metallic counterparts. Thus, the benefits of hydroelastic tailoring have not been fully exploited.

1.1 Previous Experimental Investigations

In 1998, Gowing et al. [8] presented experimental data for two hydroelastically tailored composite elliptic hydrofoils that were designed to twist under the design load. The studies showed that tip deflections reduced the effective angle of attack, which delayed cavitation inception due to reduced loading in the tip region, but the overall lift and drag characteristics remain unchanged [8]. More recently, the design, fabrication, and testing of 24-inch model-scale adaptive pitch composite marine propellers were presented in [9]. The results confirmed that a properly designed flexible composite propeller can be more efficient, and cavitation inception can be significantly delayed, when compared to its rigid counterpart in highly loaded off-design conditions and in wake inflow.

1.2 Previous Numerical Investigations

One of the first numerical studies of 3D composite marine propellers was presented in [10 & 11]. The fluid pressure and centrifugal loads were considered using PSF-2, a vortex-lattice method (VLM) developed by [12 & 13] for the hydrodynamic analysis of marine propellers subject

to steady, subcavitating (fully wetted) flows. The stress analysis was performed using ABAQUS/Standard [21], commercial FEM software. The VLM and FEM were not coupled, and thus the effect of fluid-structure interaction was not considered. A fully coupled 3D FEM/VLM (PSF-2) method was developed by [14], and used by [15] to assess the effects of stacking sequence on the hydroelastic behavior of composite propeller blades. In [16 & 17], a genetic algorithm was added to the coupled FEM/VLM procedure to determine the optimal stacking sequence of composite marine propellers. Recently, the coupled 3D FEM/VLM method was extended to study potential failure mechanisms by applying the Hanshin material failure criterion [18]. Nevertheless, all of these methods are limited to propellers operating in spatially uniform, subcavitating flow conditions. Hence, the cavitation characteristics and transient response of composite marine propellers cannot be captured.

Most recently, the author's research group has developed a 3D coupled FEM-BEM for the analysis of flexible composite propellers. The 3D BEM is a low order potential-based fluid solver developed by the hydrodynamic group at The University of Texas at Austin and the author for the hydrodynamic analysis of unsteady sheet cavitation on rigid hydrofoils, propellers, and rudders. A summary of recent developments of the BEM solver can be found in [19 & 20]. The commercial FEM package, ABAQUS/Standard [21], is used to compute the stress distributions, deformation patterns, and natural frequencies. The BEM and FEM solvers are coupled via user-defined subroutines to account for the effects of fluid-structure interaction. Extensive validation studies of the coupled BEM-FEM solver for cantilevered plate-like structures, metallic propellers in air and in water, metallic surface-piercing propellers, and self-twisting composite propellers have been presented in [22-26]. Results from the coupled BEM-FEM solver have shown good agreements with experimental measurements in terms of the circumferentially averaged blade loads, cavitation inception speeds, cavitation patterns, modal frequencies, blade deformations, as well as blade stresses.

1.3 Objective

The objective of this work is to employ the coupled BEM-FEM solver to explore the transient behavior of flexible composite propellers in uniform inflow and in wake inflow.

2 Formulation

Details of the formulation, numerical implementation, and systematic convergence and validation studies for the coupled BEM-FEM solver can be found in [24 & 26]. The formulation and solution procedure are summarized below for the sake of completeness.

In the current work, the fluid solver is formulated by decomposing the total fluid velocity, $\mathbf{v}_t$, into two parts: an effective inflow velocity, $\mathbf{v}_{in}$, obtained either by experiments or by iterating between an Euler solver and a vortex lattice method [29] which accounts for the vortical interaction between the propeller and flow field, and a perturbation velocity, $\nabla\Phi$, due to the presence of the propeller: $\mathbf{v}_t(\mathbf{x},t)=\mathbf{v}_{in}(\mathbf{x},t)+\nabla\Phi(\mathbf{x},t)$. It can be shown that the fluid problem can be reduced to a mixed-boundary value problem for the perturbation velocity potential, $\nabla^2\Phi=0$, which can be solved using a 3D BEM by applying Green's third identity. To account for the effects of fluid-structure interactions, the perturbation velocity potential is linearly decomposed into a part due to large rigid blade rotation (ϕ) and a part due to small elastic blade deformation (φ): $\Phi=\phi+\varphi$. Application of Bernoulli's formula in the rotating blade-fixed coordinate system (including the effects of centrifugal and Coriolis accelerations), the total pressure (P) can also be written in terms of the rigid blade pressure (P_r) and the elastic blade pressure (P_v) [24 & 26]:

$$P = P_r + P_v, \text{ where} \qquad (1)$$

$$P_r = P_0 + \rho\left[\frac{1}{2}|\mathbf{v}_{in}|^2 - \frac{\partial\phi}{\partial t} - \frac{1}{2}|\mathbf{v}_{in}+\nabla\phi|^2\right]$$

$$P_v = \rho\left[-\frac{\partial\varphi}{\partial t} - \mathbf{v}_{in}\cdot\nabla\varphi\right]$$

where $P_o = P_{atm} + \rho g d_s$ is the absolute hydrostatic pressure at $\boldsymbol{x}$. P_{atm} is the atmospheric pressure and d_s is the submerged depth of point $\boldsymbol{x}$ from the free surface. ρ and g are the fluid density and gravitational acceleration, respectively.

The pressure equilibrium condition at the fluid-solid interface can be satisfied by imposing the hydrodynamic pressures computed from the fluid

solver as normal tractions on the blade surface in the solid solver. Integration of the fluid pressures over the blade surface yields the equivalent nodal forces due to rigid blade rotation, $\{\mathbf{F}_h\} = \int [\mathbf{N}]^T \{\mathbf{P}_r\}\, dS$, and forces due to elastic blade deformation, $\{\mathbf{F}_v\} = \int [\mathbf{N}]^T \{\mathbf{P}_v\}\, dS$. The velocity compatibility condition at the fluid-solid interface relates the perturbation fluid velocity potential due to elastic blade deformation (φ) to the solid nodal velocities ($\dot{\mathbf{u}}$). Since $\{\mathbf{F}_v\}$ is a function of $\partial\varphi/\partial t$ and φ, the velocity compatibility condition allows $\{\mathbf{F}_v\}$ to be expressed in terms of the nodal acceleration ($\ddot{\mathbf{u}}$) and velocity ($\dot{\mathbf{u}}$):

$$\{\mathbf{F}_v\} = -[\mathbf{M_H}]\{\ddot{\mathbf{u}}\} - [\mathbf{C_H}]\{\dot{\mathbf{u}}\} \qquad (2)$$

where $[\mathbf{M}_H] = \rho \int [\mathbf{N}]^T [\mathbf{H}] [\mathbf{T}]\, dS$ and $[\mathbf{C}_H] = \rho \int [\mathbf{N}]^T [\mathbf{v}_{in} \cdot \nabla \mathbf{H}] [\mathbf{T}]\, dS$ are the added mass and hydrodynamic damping matrices, respectively. [**H**] is a geometric influence coefficient matrix, which is a function of the induced potentials due to elastic blade deformations [24 & 26].

By superimposing the added mass matrix to the structural mass matrix, [**M**], and the hydrodynamic damping matrix to the structural damping matrix, [**C**], the equilibrium equation of motion for the blades in the rotating blade-fixed coordinate system can be written as follows:

$$\begin{aligned} \left([\mathbf{M}] + [\mathbf{M}_H(t)]\right)\{\ddot{\mathbf{u}}(t)\} + \\ \left([\mathbf{C}] + [\mathbf{C}_H(t)]\right)\{\dot{\mathbf{u}}(t)\} + [\mathbf{K}]\{\mathbf{u}(t)\} = \\ \{\mathbf{F}_h(t)\} + \{\mathbf{F}_{ce}\} + \{\mathbf{F}_{co}\} \end{aligned} \qquad (3)$$

where [**K**] is the structural stiffness matrix, $\{\mathbf{u}\}$ is the nodal displacement vector, $\{\mathbf{F}_{ce}\}$ is the centrifugal force vector, and $\{\mathbf{F}_{co}\}$ is the Coriolis force vector.

In the fluid solver, the free slip boundary condition is applied on the wetted blade surface, the constant cavitation pressure (saturated vapor pressure of the liquid) condition is imposed on the cavitating surface, the pressure Kutta condition is imposed at the blade trailing edge, and the zero pressure jump condition is imposed across the zero-thickness wake surface. The wake sheet is aligned with the circumferentially averaged inflow using an iterative lifting surface method presented in [30]. An iterative process is used to determine the location, size, and shape of the moving sheet cavities by imposing the Villat-Brillouin smooth detachment condition [31 & 32] at the cavity leading edge and the zero cavity thickness condition at the cavity trailing edge. In the solid solver, the blades are assumed to be made of linear elastic anisotropic composite laminates stacked in the thickness direction. The nodes at the roots of the blades are assumed to be fixed, i.e. the blades are assumed to be rigidly attached to the hub.

The solution procedure involves application of the BEM solver to compute the hydrodynamic pressure due to rigid blades rotating in non-uniform wake ($\{\boldsymbol{P_r}\}$), and the added mass matrix ($[\mathbf{M_H}]$) and hydrodynamic damping ($[\mathbf{C_H}]$) matrix. The commercial FEM code, ABAQUS/Standard [21], is used to solve the equation of motion (Eq. 3) for the blades in the rotating blade-fixed coordinates. The BEM and FEM solvers are coupled via the use of user-defined subroutines to supply $[\mathbf{M_H}]$, $[\mathbf{C_H}]$, and $\{\boldsymbol{P_r}\}$ computed from the BEM solver to the FEM solver. The effects of large deformations are accounted for via iterations between the BEM and FEM solvers.

3 Results

To explore the hydroelastic behavior of flexible composite propellers in uniform inflow and in wake inflow, numerical predictions are compared with experimental measurements for a pair of 0.6096 m (24 in) diameter model-scale composite marine propellers. The propellers were manufactured by A.I.R. Fertigung-Technologie GmbH and designed in cooperation with the Naval Surface Warfare Center, Carderock Division (NSWCCD). The experiments were conducted at the 0.9144 m (36 in) water tunnel at NSWCCD. Details of the experimental setup, propeller design, and experimental results can be found in [9]. The composite propeller pair consists of a rigid composite propeller (5474) and a flexible composite propeller (5475). Both propellers were designed to yield the same non-dimensional thrust ($K_T = T/\rho n^2 D^4$), torque ($K_Q = Q/\rho n^2 D^5$), and efficiency ($\eta = K_T J/2\pi K_Q$) under the design condition specified by the advance coefficient ($J = V/nD$) and propeller angular frequency (n). V and D denote the propeller advance speed and diameter, respectively. The discretized geometries of the propellers are shown in Fig. 1. As shown in the figure, both propellers have six blades and share similar geometric profile.

Comparisons of the undeformed and deformed blade geometry of propellers 5474 and 5475 at the

design condition are shown in Fig. 2. As shown in the figure, the "rigid" composite (propeller 5474) is not really rigid, but it behaves as rigid in the sense that it only undergoes bending without twisting (or change in pitch). On the other hand, the flexible composite (propeller 5475) undergoes both bending and twisting, which is very obvious by comparing the undeformed and deformed geometries at the blade tip.

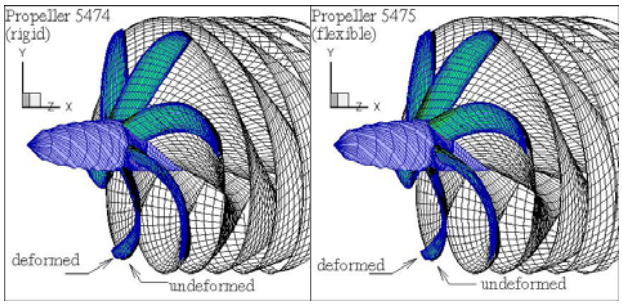

Fig. 1: Discretized geometries of the rigid (left, propeller 5474) and flexible (right, propeller 5475) composite propeller pair tested at NSWCCD.

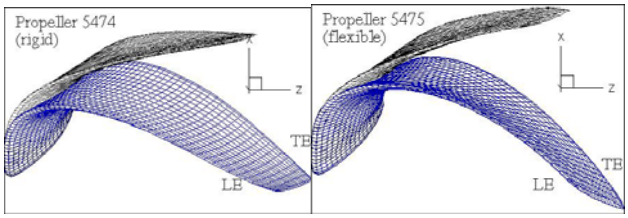

Fig. 2: Comparisons of the undeformed and deformed blade geometries of propellers 5474 and 5475 in open water flow at the design condition of J=0.66, and n=780 rpm.

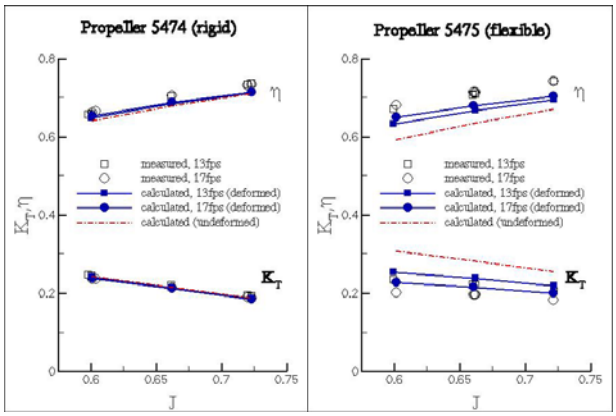

Fig. 3: Comparisons of the calculated and measured open water thrust coefficient (K_T) and efficiency (η) for propellers 5474 and 5475 at n=780 rpm.

Comparisons of the calculated and measured open water thrust coefficient (K_T) and efficiency (η) for propellers 5474 and 5475 at two different flow speeds (V=13 fps and 17fps) at n=780 rpm are shown in Fig. 3. Also shown in Fig. 3 are the computed K_T and η for both propellers without consideration for hydroelastic effects, i.e. by using the undeformed blade geometry as if the propellers were truly rigid.

The results indicate that propellers performed according to design since both the rigid (5474) and flexible (5475) composite propellers yield the same K_T and η at the design condition, J=0.66 at V=5.18 m/s (17 fps) and n=13 rev/s (780 rpm). It is important to note that the numerical predictions with consideration for hydroelastic effects (resulted denoted by calculated, deformed) compared well with experimental measurements for both propellers. In addition, it is also important to note that the difference between the calculated undeformed and deformed results is negligible for the rigid composite propeller (5474), which implies that pure bending without twisting has negligible influence on the propeller performance. On the other hand, as the calculated thrust decreases, and efficiency increases when elastic blade deformation (hydroelastic effects) is considered for the flexible composite propeller (5475). This is because the flexible composite propeller was designed to de-pitch (undergo negative twist) under the hydrodynamic load by exploiting the bending-twisting coupling effect of the anisotropic laminates. Since the deformation is load dependent, the propellers undergo more deformation as J decreases (angle of attack or load increases) and less deformation as J increases (angle of attack or load decreases). This effect can be observed in Fig. 3, where the deviation between the undeformed and deformed calculations increased with decreasing J. For the flexible composite propeller, this is equivalent to allowing the blades to automatically adjust its effective pitch distribution in off-design conditions to be closer to that under the design condition, i.e. to better align with the local flow. Hence, the efficiency of the flexible composite propeller should be higher than that of the rigid composite propeller in both under-loaded and over-loaded situations. Similarly, the efficiency of the flexible composite propeller should also be higher than that of the rigid composite propeller in wake inflow due to automatic change in the pitch distribution caused by the load-dependent bending-twisting coupling as the blades rotate in the spatially varying wake. As shown in Fig. 4, the propellers

performed as expected in both uniform inflow and wake inflow. Although small, the efficiency of the flexible composite propeller (5475) is higher than that of the rigid composite propeller (5474) for J<0.66 and J>0.66 in uniform inflow. When placed behind a four-cycle wake, the performance enhancement via the bending-twisting coupling is even more obvious when compared to the uniform inflow case since each blade can automatically change its pitch distribution to adapt to the local flow as it rotates.

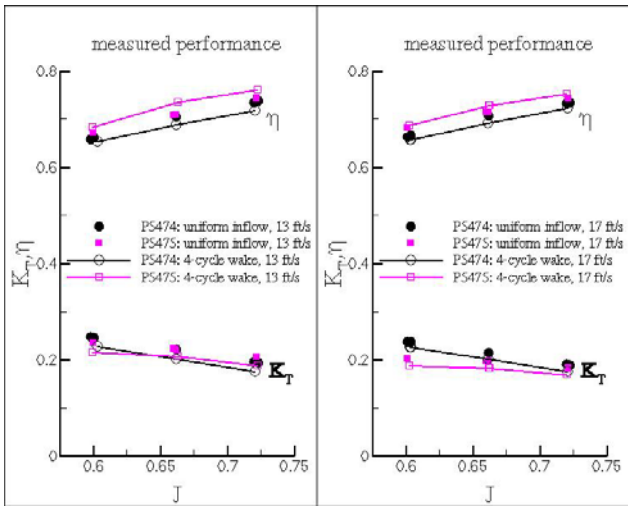

Fig. 4: Comparisons of the measured thrust coefficient (K_T) and efficiency (η) for propellers 5474 (rigid) and 5475 (flexible) at n=780 rpm in open water (uniform) flow and in wake (4-cycle wake) flow.

Due to time limitation, numerical predictions of the transient behavior of the composite propellers are not yet available. However, they will be presented in during the conference. Additional experimental validation studies of composite marine propellers can be found in [22-26].

4 Conclusions

A coupled BEM-FEM solver is presented for the numerical analysis of flexible composite propellers in uniform flow and in wake inflow. The numerical predictions are compared with experimental measurements for a rigid and flexible composite propeller pair tested at NSWCCD. Both experimental and numerical studies showed that the bending-twisting coupling behavior of anisotropic composites can be exploited to hydroelastically tailor the load-dependent blade deformations to improve the performance of composite marine propellers. Experimental results also showed that the performance improvement from the flexible composite propeller is more significant in wake inflow than in uniform inflow because each blade is allowed to automatically adjust its pitch distribution to better align itself with the local flow as it rotates through the spatially varying wake.

To fully exploit the advantages of composite marine propellers, a new design strategy is proposed in two related papers [33 & 34] in this conference. It utilizes the presented coupled BEM-FEM solver, a simplified composite plate model, and a genetic algorithm to optimize the material layering of the composite propeller. In addition, the authors' research group is also development numerical methods to investigate the effect of shock and impact loads on composite naval structures [35].

Acknowledgement

Support for this research is provided by the Office of Naval Research (Contract number N00014-05-1-0694). The authors would like to especially thank Dr. Ki-Han Kim of ONR, and Dr. Ben Chen, Dr. Richard Szwerc, and Mr. Thad Michael of NSWCCD for their support and for providing the experimental data.

References

[1] Kane, C. and Smith, J. "Composite blades in marine propulsors". *Proceedings of International Conference on Advanced Marine Materials: Technologies and Applications*, RINA, London, UK, 2003.

[2] Mouritz, A., Gellert, E., Burchill, P., and Challis, K. "Review of advanced composite structures for naval ships and submarines". *Composite Structures*, Vol. 53, pp. 21–41, 2001.

[3] Ashkenazi, Y., Gol'fman, I., Rezhkov, L., and Sidorov, N. "Glass Fiber Reinforced Plastic Parts in Ship Machinery". Leningard: Sudostroyenniye Publishing House, 1974.

[4] Pegg, R. and Reyes, H. "Progress in naval composites". *Advanced Materials and Processes*, vol. 3, pp. 35–40, 1987.

[5] Womack, S. "Carbon propller allows ships to go softly softly". *Engineer*, vol. 276, pp. 30, 1993.

[6] Kane, C. and Dow, R. "Marine propulsors design in fibre reinforced plastics". *Journal of Defense Science*, vol. 4, pp. 301–308, 1994.

[7] Searle, T. and Shot, D. "Are composite propellers the way forward for small boats". *Materials World: The Journal of the Institute of Materials*, vol. 2, no. 2, pp. 69–70, 1994.

[8] Gowing, S., Coffin, P., and Dai, C. "Hydrofoil cavitation improvements with elastically coupled composite materials". *Proceeding of 25th American Towing Tank Conference*, Iowa City, USA, 1998.

[9] Chen, B., Neely, S., Michael, T., Gowing, S., Szwerc, R., Buchler, D., and Schult, R. "Design, fabrication and testing of pitch-adapting (flexible) composite propellers". *Proceeding of The SNAME Propeller/Shafting Symposium*, Williamsburg, VA, 2006.

[10] Lin, G. "Comparative stress deflection analyses of a thickshell composite propeller blade". Technical report. David Taylor Research Center, DTRC/SHD-1373-01, December, 1991.

[11] Lin, G. "Three dimensional stress analyses of a fiber-reinforced composite thruster blade". *Proceedings of Symposium on Propellers/Shafting*. Society of Naval Architects and Marine Engineers, Virginia Beach, Virginia, September 17-18, 1991.

[12] Kerwin, J. and Lee, C.S. "Prediction of steady and unsteady marine propeller performance by numerical lifting surface theory". *Transactions of SNAME*, vol. 86, 1978.

[13] Greeley, D. and Kerwin, J. "Numerical methods for propeller design and analysis in steady flow". *Transactions of SNAME*, vol. 90, 1982.

[14] Lin, H. and Lin, J. "Nonlinear hydroelastic bebavior of propellers using a finite-element method and lifting surface theory". *Journal of Marine Science and Technology,* vol. 1, pp.114-124, 1996.

[15] Lin, H. and Lin, J. "Effect of stacking sequence on the hydroelastic behavior of composite propeller blades". *Proceedings of Eleventh International Conference on Composite Materials*. Australian Composite Structures Society, Gold Coast, Australia, July 14-18 1997.

[16] Lee, Y. and Lin, C. "Optimized design of composite propeller". *Mechanics of Advanced Materials and Structures*, vol. 11, pp.17-30, 2004.

[17] Lin, C. and Lee, Y. "Stacking sequence optimization of laminated composite structures using genetic algorithm with local improvement". *Composite Structures,* vol. 63, pp.339-345, 2004.

[18] Hashin, Z. "Failure Criteria for Unidirectional Fiber Composites*". Journal of Applied Mechanics*, Vol.47, pp.329-334, 1980.

[19] Young, Y.L. and Kinnas, S.A. "Application of BEM in the Modeling of Supercavitating and Surface-Piercing Propeller Flows," *Journal of Computational Mechanics*, Vol. 32, No. 5-6, pp. 269-280, 2003.

[20] Kinnas, S., Young, Y., Lee, H., Gu, H., and Natarajan, S. "Prediction of cavitating flow around single or two-component propulsors, ducted propellers, and rudders". *Proceedings of RINA CFD 2003: CFD Technology in Ship Hydrodynamics Conference*. London, UK, Feb. 6-7, 2003.

[21] ABAQUS, Inc., "ABAQUS Version 6.6 Documentation". ABAQUS, Inc., USA, 2006.

[22] Young, Y.L. "Hydroelastic response of composite marine propeller". *Proceedings of The SNAME Propeller/Shafting Symposium,* Williamsburg, VA. 2006.

[23] Young, Y.L. "Numerical and experimental investigations of composite marine propellers". *Proceedings of Twenty-Sixth Symposium on Naval Hydrodynamics*, Rome, Italy. 2006.

[24] Young, Y.L. "Time-dependent hydroelastic analysis of cavitating propulsors". *Journal of Fluids and Structures*, Vol. 23(2), pp. 269-295, 2007.

[25] Young Y.L., Liu Z., "Hydroelastic tailoring of composite naval propulsors". *26th International Conference on Offshore Mechanics and Arctic Engineering.* San Diego, CA. 2007.

[26] Young, Y.L., "Hydroelastic Behavior of Flexible Composite Marine Propellers in Cavitating Flow". Submitted to *Journal of Fluids and Structures*.

[27] Young, Y.L. and Kinnas, S.A. "Numerical Modeling of Supercavitating Propeller Flows," *Journal of Ship Research*, Vol. 47, pp. 48-62, 2003.

[28] Young, Y.L. and Kinnas, S.A. "Performance Prediction of Surface-Piercing Propellers," *Journal of Ship Research*, Vol. 48, No. 4, pp. 288-305, 2004.

[29] Kinnas, S., Choi, J., Lee, H., and Young, J. "Numerical Cavitation Tunnel". *Proceedings of NCT50, International conference on Propeller Cavitation*, Newcastle upon Tyne, England, April 3-5, 2000.

[30] Greeley, D. and Kerwin, J. "Numerical Methods for Propeller Design and Analysis in Steady Flow". *Society of Naval Architects and Marine Engineers Transactions*, Vol. 90, pp. 415-453, 1982.

[31] Brillouin, M. "Les surfaces de glissement de Helmholtz et la resistance des fluids". *Annales de Chimie and de Physique*, Vol. 23, pp. 145-230, 1911.

[32] Villat, H. "Sur la validite des solutions de certain problem d'hydrodynamique". *Journal de Mathematiques*, Vol. 6, No. 10, pp. 231-290, 1914.

[33] Liu, Z. and Young, Y.L. "Utilization of Deformation Coupling in Self-Twisting Composite Propellers", *16th International Conference on Composite Materials*, Kyoto, Japan, 2007.

[34] Plucinski, M.M., Young, Y.L., and Liu, Z. "Optimization of a Self-Twisting Composite Marine Propeller Using Genetic Algorithms", *16th International Conference on Composite Materials*, Kyoto, Japan, 2007.

[35] Xie, W.F., Liu, Z. and Young, Y.L. "Numerical Investigation of Shock Impact on Composite Materials", *16th International Conference on Composite Materials*, Kyoto, Japan, 2007.